Enhanced photoresponsivity of multilayer MoS_2 transistors using high work function MoO_x overlayer

Geonwook Yoo, Seongin Hong, Junseok Heo, and Sunkook Kim

Citation: Appl. Phys. Lett. **110**, 053112 (2017); doi: 10.1063/1.4975626
View online: http://dx.doi.org/10.1063/1.4975626
View Table of Contents: http://aip.scitation.org/toc/apl/110/5
Published by the American Institute of Physics

Articles you may be interested in

Improved integration of ultra-thin high-k dielectrics in few-layer MoS2 FET by remote forming gas plasma pretreatment
Appl. Phys. Lett. **110**, 053110053110 (2017); 10.1063/1.4975627

Chemical vapor deposition of monolayer MoS2 directly on ultrathin Al2O3 for low-power electronics
Appl. Phys. Lett. **110**, 053101053101 (2017); 10.1063/1.4975064

Encapsulation of graphene in Parylene
Appl. Phys. Lett. **110**, 053504053504 (2017); 10.1063/1.4975491

Ultrafast photocurrent measurements of a black phosphorus photodetector
Appl. Phys. Lett. **110**, 051102051102 (2017); 10.1063/1.4975360

RIGHTSLINK

APPLIED PHYSICS LETTERS **110**, 053112 (2017)

CrossMark

Enhanced photoresponsivity of multilayer MoS_2 transistors using high work function MoO_x overlayer

Geonwook Yoo,[1,a)] Seongin Hong,[2] Junseok Heo,[3] and Sunkook Kim[2,a)]
[1]School of Electronic Engineering, Soongsil University, Seoul 06938, South Korea
[2]School of Advanced Materials Science & Engineering, Sungkyunkwan University, 300, Chunchun-dong, Jangan-gu, Suwon, 16419, South Korea
[3]Department of Electrical and Computer Engineering, Ajou University, Suwon 16499, South Korea

(Received 1 December 2016; accepted 24 January 2017; published online 3 February 2017)

Using thin sub-stoichiometric molybdenum trioxide (MoO_x, $x < 3$) overlayer, we demonstrate over 20-folds enhanced photoresponsivity of multilayer MoS_2 field-effect transistor. The fabricated device exhibits field-effect mobility (μ_{FE}) of up to 41.4 cm^2/V s and threshold voltage (V_{TH}) of −9.3 V, which is also modulated by the MoO_x overlayer. The MoO_x layer (∼25 nm), commonly known for a high work function (∼6.8 eV) material with a band gap of ∼3 eV, is evaporated on top of the MoS_2 channel and confirmed by the transmission electron microscope analysis. The electrical and optical modulation effects are associated with interfacial charge transfer and thus an induced built-in electric field at the MoS_2/MoO_x interface. The results show that high work function MoO_x can be a promising heterostructure material in order to enhance the photoresponse characteristics of MoS_2-based devices. *Published by AIP Publishing.*
[http://dx.doi.org/10.1063/1.4975626]

Molybdenum disulfide (MoS_2), a two-dimensional transition metal dichalcogenide, has been considered a promising candidate for emerging optoelectronic devices.[1–6] MoS_2 possesses unique and advantageous properties such as controllable bandgap energy from a direct (1.2 eV) to indirect band gap (1.8 eV) depending on the number of layers,[7] high mobility (∼200 cm^2/V s) with a high-k dielectric layer,[1,8] and high absorptivity.[9] Especially, the existing bandgap allows low-dark current by modulating MoS_2 channel to depletion, which is suitable for a phototransistor mode. Furthermore, its outstanding mechanical property enlarges the application to flexible and conformable photodetectors for wearable devices,[10,11] and the recent advances in scalable and large-area process of TMDCs (Transition Metal Dichalcogenides) make these unique features more compelling toward image sensor.[12–14]

In this sense, intensive research efforts have been devoted to improve figure-of-merits (e.g., responsivity and spectral response) of MoS_2-based photodetectors by adopting a surface plasmonic nanostructure,[15] a unique device structure,[16] and various organic and inorganic overlayers;[17–20] For example, the p-type PbS quantum-dots, p-type organic semiconductors (e.g., copper phthalocyanine, rubrene), organic dye, and hafnium oxide were investigated as a stacking layer on the top of MoS_2, resulting in enhanced photoresponsivity (R). Meanwhile, various p-n junctions based on MoS_2 heterostructure are also suggested for enhanced photodetection characteristics.[21–23] Considering desirable properties for an overlayer, molybdenum trioxide (MoO_x) can be a good alternative in that MoO_x possess a large bandgap (∼3 eV) and is more stable compared with organic materials in ambient conditions.[24–26] In addition, a high work function of evaporated MoO_x (6.6–6.8 eV) layer allows modulating of electronic property of MoS_2 field-effect transistor (FET).[27] In this study, we present multilayer MoS_2 phototransistor with an MoO_x overlayer deposited by thermal evaporation. The interface between MoS_2 and MoO_x is characterized using transmission electron microscope (TEM) with energy dispersive spectroscopy (EDS) analysis. We investigate electrical performance and photoresponsive characteristics of multilayer MoS_2 FET before and after stacking an MoO_x overlayer onto the MoS_2 channel. It is found that the photoresponsivity of the MoS_2 phototransistor with the thin MoO_x overlayer is enhanced by more than 20 times, which is associated with electron charge transfer due to the high work function of MoO_x. Finally, energy band diagram model is used to discuss the results.

Figure 1(a) shows a schematic illustration of multilayer MoS_2 transistor with an MoO_x overlayer. Mechanically exfoliated MoS_2 flakes from bulk MoS_2 crystals (Graphene Market, USA) by a conventional scotch-tape method were transferred onto a heavily doped p-type Si substrate with thermally grown 200 nm SiO_2 layer. For the source and drain (S/D) electrodes, Au (∼70 nm) was evaporated, followed by patterning using the conventional lift-off technique. Then, a thin MoO_x layer (∼25 nm) was deposited by thermal evaporation, followed by opening electrical contact using conventional photolithography and wet chemical etching. Finally, the fabricated device was annealed at 573 K in N_2 for 10 min using a rapid thermal annealing to remove any absorbed organic residues and to improve contact resistance. Figures 1(b) and 1(c) show a cross sectional TEM image of the $SiO_2/MoS_2/MoO_x$ stack and its enlarged image at the MoS_2/MoO_x interface with EDS analysis, respectively. The transition layer was ∼3.1 nm thick, in which the atomic % ratio changes clearly show the sub-stoichiometric MoO_x ($x < 3$) layer deposited on top of the multilayer MoS_2 flake. The transition layer formed due to interface mixing during thermal evaporation used in this work.

Figure 2 shows typical electrical characteristics of the fabricated device. Measured transfer curves of I_{DS}–V_{GS} for

a)Electronic addresses: gwyoo@ssu.ac.kr and kimskcnt@gmail.com

RIGHTSLINK

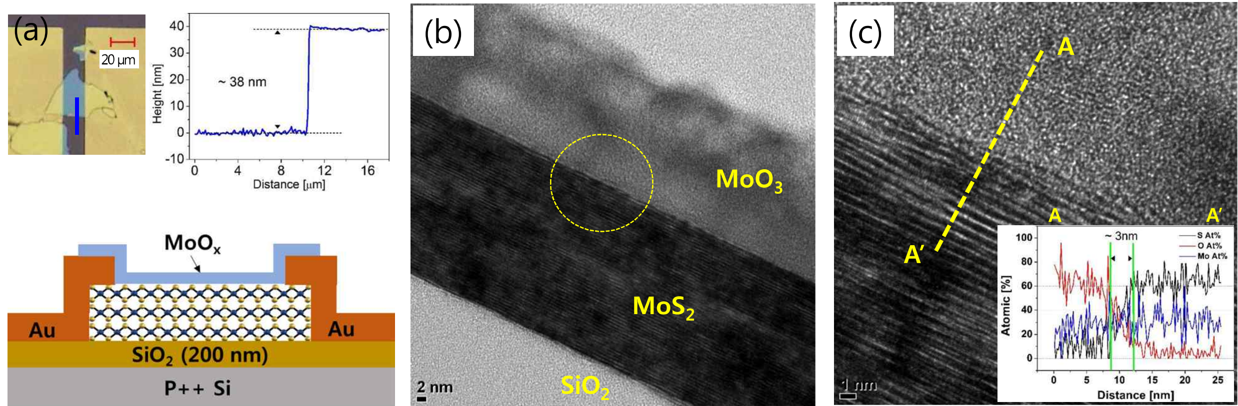

FIG. 1. (a) Schematic illustration of the multilayer MoS_2 FET with MoO_x overlayer. Thickness profile measured with AFM shows about 38 nm. (b) Cross sectional TEM image of SiO_2-MoS_2-MoO_x. (c) Enlarged TEM image of the MoS_2-MoO_x interface. EDS analysis in the inset shows the change of atomic % ratio across the transition layer of ~3 nm thickness.

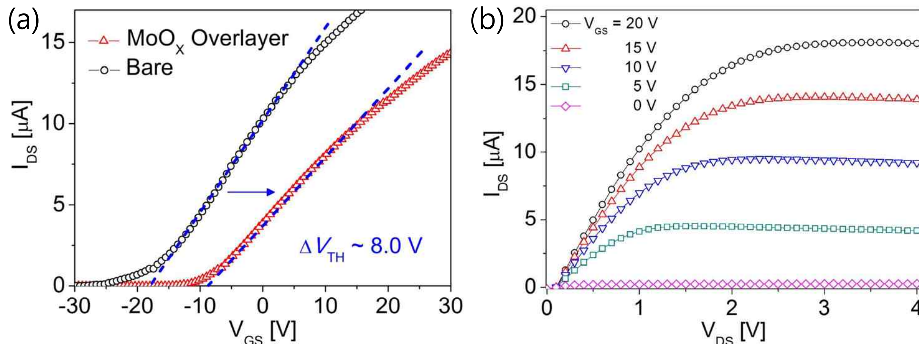

FIG. 2. (a) Transfer characteristics (I_{DS}-V_{GS}) of the fabricated MoS_2 FETs before (Bare) and after (MoO_x overlayer) stacking the MoO_x layer (25 nm) for $V_{DS} = 1$ V. (b) Output characteristics (I_{DS}-V_{DS}) of the MoS_2 FET with MoO_x overlayer for $V_{GS} = 0$, 5, 10, 15, 20 V, exhibiting good linearity at low V_{DS} and saturation at high V_{DS} conditions.

$V_{DS} = 1$ V are presented in Fig. 2(a), in which the effect of the MoO_x overlayer on V_{TH} shift ($\Delta V_{TH} \sim 8.0$ V) is clearly shown. The field-effect mobility (μ_{FE}) in a linear operation regime was extracted from $\mu_{FE} = L \cdot g_m/(W \cdot C_{OX} \cdot V_{DS})$, where W is channel width, L is channel length, C_{OX} is capacitance of SiO_2, and V_{DS} is drain bias of 1 V. Threshold voltage (V_{TH}) was calculated using a linear extrapolation method in a linear regime ($V_{DS} = 1$ V); it was found from the intercept of a tangent at the maximum g_m with V_{GS} axis. Subthreshold slope was calculated from $SS = [d(\log_{10} I_{DS})/dV_{GS}]^{-1}$. Figure 2(b) represents output characteristics (I_{DS}-V_{DS}) for $V_{GS} = 0$, 5, 10, 15, 20 V, exhibiting an ohmic-like linear behavior at low V_{DS} and saturation at high V_{DS} bias conditions. Electrical parameters are summarized in Table I. The positive ΔV_{TH} is attributed to the significant electron transferring from MoS_2 to MoO_x, resulting in the depletion of electrons in the MoS_2 channel. The average ΔV_{TH} was $\sim 7.6 \pm 0.9$ V, and its corresponding amount of depleted charge concentration after depositing MoO_x overlayer was estimated to $\Delta n \sim (0.8 \pm 0.1) \times 10^{12}$ cm^{-2} (at $V_G = 20$ V). We calculated the charge concentration (n) using parallel-capacitor model with $n = Q/e = C_{OX} \cdot (V_G - V_{TH})/e$, where C_{OX} is capacitance of SiO_2, V_G is gate-bias, V_{TH} is threshold voltage, and e is elementary charge. The reduction of μ_{FE} originated from the scattering by impurities at the intermixed interface between MoO_x and MoS_2, and from the depleted charge concentration in the channel. The increased SS indicates that interface trap density at the intermixed interface increased as well. More details with energy band diagram will be discussed in the following.

TABLE I. Electrical parameters and photoresponsivity (R) of the fabricated MoS_2 FETs before and after stacking MoO_x layer. R was extracted at $V_{GS} = -30$ V and optical power density of 8.6 mW/cm^2.

	V_{TH} (V)	μ_{FE} (cm^2/V s)	SS (V/dec)	R (A/W)
Before	−17.3	62.1	1.8	3.5
After	−9.3	41.4	3.2	65.2

We investigated photoresponsive characteristics of the multilayer MoS_2 phototransistor before (w/o MoO_x) and after (w/ MoO_x) stacking the MoO_x layer on top of the MoS_2 channel. Figure 3(a) shows power-dependent photoresponsivity (R) for various irradiances (8.6, 17.2, 34.4, 68.7, 137.5, 274.9 mW/cm^2) as well as gate-bias ($V_{GS} = -30$ to -10 V, 5 V step) conditions under an incident light wavelength (λ) of 532 nm. The photoresponsivity was calculated from $R = I_{ph}/P_{inc}$, where I_{ph} ($= I_{DS} - I_{dark}$) is photocurrent and P_{inc} is incident optical power. Two typical characteristics were observed for both bare (w/o MoO_x) and MoO_x overlayered MoS_2 (w/ MoO_x) devices; photoresponsivity was reduced with increasing irradiance as well as gate modulation (V_{GS}) due to a trap-dominated process.[18] In order to characterize photoswitching behavior of the devices, we measured temporal photoresponses at $V_{DS} = 1$ V with a pulsed laser at 638 nm. Photocurrents generated and recombined in accordance with the incident light, turning on and off at a period of 20 s. The observed temporal responses throughout the multiple cycles demonstrate a stable and constant

RIGHTSLINK

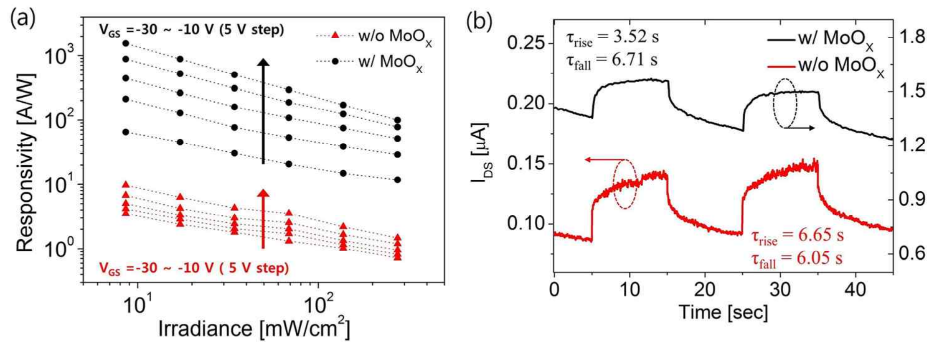

FIG. 3. Comparison of photoresponse characteristics of the multilayer MoS_2 FET before (w/o MoO_x) and after stacking the MoO_x layer (w/MoO_x). (a) Power-dependent responsivity for various V_{GS} bias from −30 V to −10 V at an illumination wavelength of 532 nm and V_{DS} = 1 V. (b) Temporal photoresponse behaviors at V_{DS} = 1 V with pulsed laser at 638 nm and 8.6 mW/cm^2, which is turned on and off every 10 s.

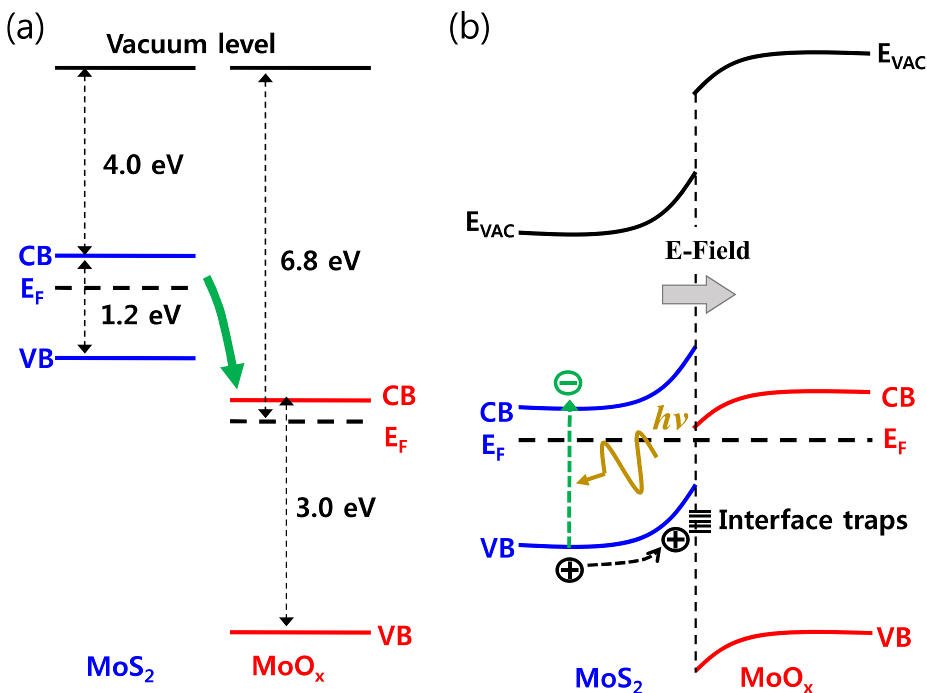

FIG. 4. Energy band diagram for multilayer MoS_2 with an MoO_x overlayer. (a) Significant interfacial electrons transfer from MoS_2 to MoO_x when physical contact formed. (b) At equilibrium, induced band bending at the interface leads to built-in electric-field, contributing electron-hole pair dissociation.

photoswitching performance of the device. In particular, the response times (i.e., rise and fall time) were calculated from 10% to 90%, and 90% to 10% of the maximum photocurrent after light was turned on and off, respectively. After stacking MoO_x layer, the rise time (τ_{rise}) decreased from 6.65 s to 3.52 s while the fall time (τ_{fall}) remained similar. It is to be noted that the photoresponsivity is enhanced by more than 20-folds with enhanced switching characteristics for the measured irradiance and V_{GS} ranges.

Aforementioned V_{TH} shift and enhanced photoresponsivity by stacking thin MoO_x overlayer can be explained using the energy-band diagram. It is commonly considered that evaporated MoO_x films have a very high work function of 6.6–6.8 eV and a bandgap of ∼3 eV.[24–26] Note that the incident light wavelengths (532 nm and 638 nm) are not absorbed in the MoO_x overlayer due to its large bandgap (∼3 eV). As presented in Fig. 4(a), when MoS_2 and MoO_x form a physical contact, a significant electron charges transfer from MoS_2 to MoO_x because the energy levels of MoO_x including Fermi level (E_F) and conduction band (CB) locate below the valence band (VB) of MoS_2. Consequently, significant interfacial charge transfer occurs and electron charges deplete in MoS_2 (i.e., less accumulated charges), and thus V_{TH} shift toward positive direction. Meanwhile, the interfacial charge transfer can induce upward band-bending in MoS_2 and downward in MoO_x at equilibrium, as shown in Fig. 4(b). Thus, an induced built-in electric field can effectively separate photo-generated electron-hole pairs in MoS_2 and contribute to the holes to be trapped at the interface trap sites instead of electron-hole recombination. Therefore, photoresponsivity of the multilayer MoS_2 phototransistor could be enhanced by more than 20 times at V_{GS} = −30 V by stacking the MoO_x overlayer.

In conclusion, we have reported on electrical and photoresponsive characteristics of the multilayer MoS_2 FET with the evaporated thin MoO_x overlayer. The fabricated device exhibits μ_{FE} of up to 41.4 cm^2/V s and threshold voltage of −9.3 V, which was positive-shifted from −17.3 V. Furthermore, the MoO_x overlayer results in enhanced photoresponsivity of more than 20 times (65.2 A/W) at V_{GS} = −30 V under the illumination of 532 nm and 8.5 mW/cm^2. The modulation of electrical as well as optical properties is associated with the high work function of evaporated MoO_x layer contributing to the significant interfacial electron charge transfer from the MoS_2 channel to MoO_x and thus induced built-in electric field at the MoS_2/MoO_x interface. The large bandgap of MoO_x can be an

RIGHTSLINK

additional merit as an overlayer to be transparent to visible light. The results suggest that photoresponsive characteristics of the multilayer MoS_2 phototransistor can be greatly improved by integrating an inorganic layer, MoO_x, with high work function, and can further be a promising heterostructure for high performance phototransistors based on MoS_2 and other 2-D materials.

This research was supported in part by the National Research Foundation of Korea (NRF) funded by the Ministry of Science, ICT, and Future Planning (Grant No. NRF-2014M3A9D7070732).

[1]Q. H. Wang, K. Kalantar-Zadeh, A. Kis, J. N. Coleman, and M. S. Strano, Nat. Nanotechnol. **7**, 699 (2012).
[2]O. Lopez-Sanchez, D. Lembke, M. Kayci, A. Radenovic, and A. Kis, Nat. Nanotechnol. **8**, 497 (2013).
[3]F. H. L. Koppens, T. Mueller, P. Avouris, A. C. Ferrari, M. S. Vitiello, and M. Polini, Nat. Nanotechnol. **9**, 780 (2014).
[4]M. Buscema, J. O. Island, D. J. Groenendijk, S. I. Blanter, G. A. Steele, H. S. J. van der Zant, and A. Castellanos-Gomez, Chem. Soc. Rev. **44**, 3691 (2015).
[5]W. Choi, M. Y. Cho, A. Konar, J. H. Lee, G.-B. Cha, S. C. Hong, S. Kim, J. Kim, D. Jena, J. Joo, and S. Kim, Adv. Mater. **24**, 5832 (2012).
[6]Z. Yin, H. Li, H. Li, L. Jiang, Y. Shi, Y. Sun, G. Lu, Q. Zhang, X. Chen, and H. Zhang, ACS Nano **6**, 74 (2012).
[7]K. F. Mak, C. Lee, J. Hone, J. Shan, and T. F. Heinz, Phys. Rev. Lett. **105**, 136805 (2010).
[8]L. Liu, S. B. Kumar, Y. Ouyang, and J. Guo, IEEE Trans. Electron Devices **58**, 3042 (2011).
[9]R. Ganatra and Q. Zhang, ACS Nano **8**, 4074 (2014).
[10]D. Akinwande, N. Petrone, and J. Hone, Nat. Commun. **5**, 5678 (2014).
[11]R. Cheng, S. Jiang, Y. Chen, Y. Liu, N. Weiss, H.-C. Cheng, H. Wu, Y. Huang, and X. Duan, Nat. Commun. **5**, 5143 (2014).
[12]Y.-H. Lee, X.-Q. Zhang, W. Zhang, M.-T. Chang, C.-T. Lin, K.-D. Chang, Y.-C. Yu, J. T.-W. Wang, C.-S. Chang, L.-J. Li, and T.-W. Lin, Adv. Mater. **24**, 2320 (2012).
[13]Y. Zhan, Z. Liu, S. Najmaei, P. M. Ajayan, and J. Lou, Small **8**, 966 (2012).
[14]J. Jeon, S. K. Jang, S. M. Jeon, G. Yoo, Y. H. Jang, J.-H. Park, and S. Lee, Nanoscale **7**, 1688 (2015).
[15]J. Miao, W. Hu, Y. Jing, W. Luo, L. Liao, A. Pan, S. Wu, J. Cheng, X. Chen, and W. Lu, Small **11**, 2392 (2015).
[16]J. Kwon, Y. K. Hong, G. Han, I. Omkaram, W. Choi, S. Kim, and Y. Yoon, Adv. Mater. **27**, 2224 (2015).
[17]S. H. Yu, Y. Lee, S. K. Jang, J. Kang, J. Jeon, C. Lee, J. Y. Lee, H. Kim, E. Hwang, S. Lee, and J. H. Cho, ACS Nano **8**, 8285 (2014).
[18]D. Kufer and G. Konstantatos, Nano Lett. **15**, 7307 (2015).
[19]D. Kufer, I. Nikitskiy, T. Lasanta, G. Navickaite, F. H. L. Koppens, and G. Konstantatos, Adv. Mater. **27**, 176 (2015).
[20]J. Pak, J. Jang, K. Cho, T.-Y. Kim, J.-K. Kim, Y. Song, W.-K. Hong, M. Min, H. Lee, and T. Lee, Nanoscale **7**, 18780 (2015).
[21]L. Hao, Y. Liu, W. Gao, Z. Han, Q. Xue, H. Zeng, Z. Wu, J. Zhu, and W. Zhang, J. Appl. Phys. **117**, 114502 (2015).
[22]E. W. Lee, C. H. Lee, P. K. Paul, L. Ma, W. McCulloch, S. Krishnamoorthy, Y. Wu, A. Arehart, and S. Rajan, Appl. Phys. Lett. **107**, 103505 (2015).
[23]H. Jeong, S. Bang, H. M. Oh, H. J. Jeong, S.-J. An, G. H. Han, H. Kim, K. K. Kim, J. C. Park, Y. H. Lee, G. Lerondel, and M. S. Jeong, ACS Nano **9**, 10032 (2015).
[24]M. T. Greiner, M. G. Helander, W.-M. Tang, Z.-B. Wang, J. Qiu, and Z.-H. Lu, Nat. Mater. **11**, 76 (2012).
[25]Y. Zhao, J. Chen, W. Chen, and D. Ma, J. Appl. Phys. **111**, 043716 (2012).
[26]C. Battaglia, X. Yin, M. Zheng, I. D. Sharp, T. Chen, S. McDonnell, A. Azcatl, C. Carraro, B. Ma, R. Maboudian, R. M. Wallace, and A. Javey, Nano Lett. **14**, 967 (2014).
[27]J. Lin, J. Zhong, S. Zhong, H. Li, H. Zhang, and W. Chen, Appl. Phys. Lett. **103**, 063109 (2013).

RIGHTSLINK